Adaptive Fuzzy Clustering Algorithm for Segmentation of Biomedical Colour Images

Daan Zhu, Kate H. Sullivan and Stamatis N. Pagakis

Abstract— **In this paper, we describe the application of an adaptive fuzzy clustering algorithm to the segmentation of colour biomedical images. In comparison to traditional colour image segmentation algorithms, the advantage of this algorithm is intelligent location of a range of chosen colours (ROC) based on a manually selected reference colour. The colours within the ROC have similar colour properties in terms of hue, saturation and intensity. The size of colour range is based on an adaptive Lagrange parameter λ. Experimental results prove that this adaptive fuzzy clustering algorithm gives better segmentation results than non-adaptive fuzzy clustering algorithms.**

I. Introduction

BIOMEDICAL image segmentation is an important step in image analysis and is a prerequisite for feature extraction or shape analysis. Segmentation algorithms can be based on statistical models [11], graph-based models [8], morphological filters [7] etc. In this paper, we describe the application of an adaptive fuzzy clustering algorithm to the segmentation of biomedical colour images. Biomedical images and especially the microscopy images that we are dealing with, are complex and difficult to analyse. The regions of interest are small with fuzzy, undefined edges so that traditional techniques cannot be easily applied.

Fuzzy algorithms were developed and successfully implemented for several applications such as colour lip image segmentation [1] or medical diagnostic systems [10]. Pham [2] used an adaptive fuzzy c-means algorithm to segment gray magnetic resonance images. This is a multigrid-based algorithm used to remove shading artifacts. Puzicha et al. [4] analysed a histogram distribution and used a pairwise term to segment images. However the results of segmentation relied on a generative statistical model before classification. Fuzzy algorithms have also been used for colour image segmentation. Deng et al. [12] used a fuzzy algorithm to quantize colour into several colour classes representing the different regions in an image. The original image colours were then replaced pixel by pixel, with their corresponding colour class labels, thus forming a class-map of the image. More colour classes produce a more accurate representation of the original image. However, too many classes create a serious problem if segmentation of one specific part of the image is required, which is usually the case in histological images. The same object in the segmented image will be represented by more than one colour class and thus the automatic segmentation becomes difficult and impractical to achieve. The traditional fuzzy c-means algorithm (FCM) [3] and most of the modified FCM find the colour centroids and the corresponding colour classes globally. Using this method, at least 30 colour classes were needed to have a reasonable representation of our histological images.

Acknowledgement: We would like to thank Dr. Stelios Psarras at the Foundation for Biomedical Research of the Academy of Athens for providing the sample images and the manual segmentation data.

Adaptive fuzzy clustering algorithms (AFCA) have been used previously to segment biomedical images. Dave and Bhaswan [9] used AFCA to detect the feather of ellipses and the performance results were compared using the Hough transform. However, it appears that there have been no attempts to use adaptive fuzzy methodology for the segmentation of colour histological images. There are 16 million different colours in a true colour image (three colours, 8-bit channels). An efficient algorithm to classify the colours of interest is essential for the biologist.

In this paper, we present a novel adaptive fuzzy clustering algorithm (AFCA). There are two differences between our AFCA and other traditional fuzzy algorithms. Firstly, our AFCA makes a local clustering analysis instead of a global fuzzy clustering analysis, as in most FCM applications. Secondly, a Lagrange parameter (λ) is used to regularise a manually defined reference colour. Our algorithm approaches optimum class centroids through an adaptive step. Under this regularisation only the colour centroids which have similar colour properties to the reference colours are selected.

II. Method and Mathematical Formulation

A. Colour models

Before the derivation of the AFCA, we need to introduce the colour models. Colour models are mathematical representations of a set of colours. The most popular models are RGB, HSI and HSB. The well known RGB (Red, Green Blue) model is used by most visualisation systems and is based on a Cartesian coordinate system under a cube subspace. In this cube the RGB values are at three corners; and the CMY (Cyan, Magenta, Yellow) are at the others.

The Hue-Saturation-Intensity (HSI) model defines a colour space in terms of three constituent components. It is a nonlinear transformation of the RGB colour space. In this model, H describes a pure colour, S measures the degree to which a pure colour is diluted with white light. The HSI colour model is represented by a double prism subspace based on the Maxwell triangle generated by the RGB cube subspace. The transform and inverse transform from RGB to HSI space is given below

$$I = \frac{R+G+B}{3} \tag{1}$$

$$S = 1 - (3 \times \frac{min(R,G,B)}{R+B+G}) \tag{2}$$

$$H = cos^{-1}\frac{0.5 \times (2R - G - B)}{\sqrt{(R-G)^2 + (R-B) \times (G-B)}} \quad (3)$$

If $B > G$ then $H = 2 \times \pi - H$ and if $R = G = B$ then H is undefined and $S = 0$. The ranges for each colour channel are $0 \leq H \leq 2\pi$, $0 \leq S \leq 1$ and $0 \leq I \leq 1$. The inverse RGB to HSI transform is summarised below
If $H = -1$ R=G=B=I;
If $H < \frac{2\pi}{3}$

$$R = \frac{3 + 3S \cdot \cos(H)}{\cos(\frac{\pi}{3} - H)} \quad (4)$$
$$G = 1 - (B + R) \quad (5)$$
$$B = \frac{1 - S}{3} \quad (6)$$

If $H < \frac{4\pi}{3}$, *then* $H^{'} = H - \frac{2\pi}{3}$

$$R = \frac{1 - S}{3} \quad (7)$$
$$G = \frac{3 + 3S \cdot \cos(H^{'})}{\cos(\frac{\pi}{3} - H^{'})} \quad (8)$$
$$B = 1 - (G + R) \quad (9)$$

If $H < 2\pi$, *then* $H^{'} = H - \frac{4\pi}{3}$

$$R = 1 - (G + B) \quad (10)$$
$$G = \frac{1 - S}{3} \quad (11)$$
$$B = \frac{3 + 3S \cdot \cos(H^{'})}{\cos(\frac{\pi}{3} - H^{'})} \quad (12)$$

New RGB values need to be normalised and adjusted to a proper display range.

The third colour model is Hue-Saturation-Brightness (HSB), sometimes called Hue-Saturation-Value (HSV) and is similar to HSI. HSB is a nonliner transformation of the RGB colour space. The forward and inverse transforms from RGB to HSB are shown below

$$H = \begin{cases} 60 \times \frac{G-B}{max-min} + 0 & max = R \ \ and \ \ G \geq B \\ 60 \times \frac{G-B}{max-min} + 360 & max = R \ \ and \ \ G < B \\ 60 \times \frac{B-R}{max-min} + 120 & max = G \\ 60 \times \frac{R-G}{max-min} + 240 & max = B \end{cases} \quad (13)$$

$$S = \frac{max - min}{max} \quad (14)$$
$$V = max \quad (15)$$

where *max* and *min* equal the maximum and minimum of (R,G,B) values. In real practice if $max = min$, then $S = 0$ and H is undefined and if $max = 0$ then $v = 0$ and S is undefined.

The inverse transform from RGB to HSB is shown

$$H_i = [\frac{H}{60}] mod 6 \quad (16)$$

$$f = [\frac{H}{60}] - H_i \quad (17)$$

$$p = V(1 - S) \quad (18)$$

$$q = V(1 - fS) \quad (19)$$

$$t = V(1 - (1 - f)S) \quad (20)$$

- if $H_i = 0$ then $R = V, G = t$ and $B = p$
- if $H_i = 1$ then $R = q, G = V$ and $B = p$
- if $H_i = 2$ then $R = p, G = V$ and $B = t$
- if $H_i = 3$ then $R = p, G = q$ and $B = V$
- if $H_i = 4$ then $R = t, G = p$ and $B = V$
- if $H_i = 5$ then $R = V, G = p$ and $B = q$

In our work, microscopy images are converted from RGB to HSI or HSB. After finding the optimum colour centroids in the HSI or HSB colour space, an inverse transform is applied using the above equations to covert the image into RGB colour space. Our data indicates that segmentation processed in either the HSB or HSI gives similar results.

B. Adaptive Fuzzy C-means algorithm

Before the introduction of an Adaptive Fuzzy C-means algorithm (AFCA), the application of a traditional fuzzy C-means algorithm (FCA) on our images is discussed. FCM is used in special cases to obtain a segmentation via fuzzy pixel classification. Unlike hard classification methods which force pixels to belong exclusively to one class, FCM allows pixels to belong to multiple classes with varying degrees of membership. These algorithms were commonly used to segment magnetic resonance images and correct the shading effect. The standard FCM algorithm for scalar data seeks the membership functions u_k and centroids v_k, such that the following objective function is minimised:

$$J_{FCM} = \sum_{i,j} \sum_{k=1}^{C} u_k(i,j)^q \|x(i,j) - v_k\|^2 \quad (21)$$

where $u_k(i,j)$ is the membership value at pixel location (i,j) for class k such that $\sum_{k=1}^{C} = 1$, $x(i,j)$ is the observed image intensity at location (i,j), and v_k is the centroid of class k. The total number of classes C is normally defined in advance. The parameter q is a weighting exponent on each fuzzy membership and determines the value of fuzzy classification and $q > 1$. In most applications $q = 2$. Equation (21) denotes the grey scale image segmentation. In this work, the images we processed are true colour images. To consider the colour channels, the above equation will become

$$J_{FCM} = \sum_{i,j} \sum_{k=1}^{C} u_k(i,j)^q \|x_l(i,j) - v_{l,k}\|^2 \quad (22)$$

where l are the colour channels, $1 \leq l \leq 3$. Equation (22) is the partition FCM algorithm. The norm operator $\|\cdot\|^2$ represents the standard Euclidean distance which means the distance of the current pixel values (three channels) to the current centroid point. If we introduced a reference colour into our fuzzy equation, the equation (22) becomes

$$J_{AFCA} = \sum_{i,j}\sum_{k=1}^{C} u_k(i,j)^q \|x_l(i,j) - v_{l,k}\|^2 + \lambda\|\tilde{x_l} - v_{l,k}\|^2 \tag{23}$$

where λ is the Lagrange parameter used to regularise the reference colour in the global classification sets. $\tilde{x_l}$ is the reference colour point. The selection of λ is an adaptive step. The reference colour is selected by the user before the classification.

C. Iterative solution

Pham et al. [2] developed an iterative step for AFCA. The objective function (23) can be minimised in a fashion similar to the standard FCM algorithm. Taking the first derivatives of J_{AFCA} with respect to $u_k(i,j)$, $v_{l,k}$ and $\tilde{x_l}$ and setting them equal to zero results in three necessary conditions for J_{AFCA} to be at a minimum. Using these conditions, the steps for our AFCA algorithm can then be described as follows:

1 Manually select of a reference colour and convergence tolerance ε.

2 Set number of centroids and initial values for the membership matrix, $v_{l,k}, k = 1, \cdots, C$

3 Compute membership matrix as follows:

$$u_k(i,j) = [\sum_{m=1}^{c} \frac{\|x(i,j) - v_{l,k}\|}{\|x(i,j) - v_{l,m}\|}^{\frac{2}{m-1}}]^{-1} \tag{24}$$

for all (i,j) and $k = 1, \cdots, c$; and $l = 1, \cdots, 3$.

4 Update new centroids:

$$v_{l,k} = \frac{\sum_{k=1}^{c} u_k(i,j)^m \cdot x_l(i,j)}{\sum_{k=1}^{c} u(i,j)^m} + \lambda \cdot \frac{\sum_{k=1}^{c} u_k(i,j)^m \cdot \tilde{x_l}}{\sum_{k=1}^{c} u(i,j)^m} \tag{25}$$

where $l = 1, \cdots, 3$.

5 Calculate each iterative error.
The error calculations can be approached in two ways. The simplest approach is calculation of the iterative convergence.

$$Error_{t+1}(v) = \sum_{k=1}^{c}\sum_{l=1}^{3} \|v_{l,k}^{(t+1)} - v_{l,k}^{(t)}\|^2 \tag{26}$$

where t denotes the iterations. Another approach to the convergence error is by calculating the Euclidean distances between the values $x_k(i,j)$ and the centroid $v_{l,k}$ in the same classified class.

$$Error_{t+1}(v) = \sum_{k=1}^{c} \|x_k(i,j)^{(t+1)} - v_{l,k}^{(t+1)}\|^2 \tag{27}$$

6 If the $Error < \varepsilon$, the iteration is converged, then quit. Otherwise, go to step 3.

In practice, the membership matrix u is initialised randomly, see step 2. The row of membership matrix must be normalised by their sum. The initial membership matrix cannot always guarantee to obtain the optimum centroids which is one of the disadvantages of using FCM. In step 5, we use two different ways to calculate the iterative errors, equations 26 and 27. By using equation 26, the error is calculated by getting its Euclidean distance between the current and previous centroids. In this calculation, the error always converges under any of the conditions. However difficulties arise using equation 27 as a stop criterion. The optimum solution of FCM and AFCA depends on the initial membership matrix u and the number of centroids. In some cases, if the FCM or AFCA cannot get a set of optimum centroids, in other words equation 27 will never reach convergence tolerance, the iteration will never stop. In practice, equation 26 is used to decide that the iterations can be stopped and equation 27 can be used to judge whether the iteration can give a set of optimum centroids.

D. λ calculation

λ is a Lagrange parameter which is used to constrain the colour under the regularisation of the reference colour. If λ is zero, AFCM degrades to FCM. The calculation of λ is an adaptive step based on the result of previous iterative centroids. Pham and Jerry [2] introduced two regularisation terms and two Lagrange parameters to control two terms in the AFCA. Two λs in their application are fixed. In our work, the value of λ will be adjusted based on the previous iterations. This criterion provides the basis for the method used to select λ. With increasing number of iterations the value of λ should converge to a small positive value. Calculation of λ leads to

$$\lambda = \frac{\sum_{i,j}\sum_{k=1}^{C} u_k(i,j)^q \|x_l(i,j) - v_{l,k}\|^2}{\|\tilde{x_l} - v_{l,k}\|^2} \tag{28}$$

This calculation is self-adapting. If the iteration converges to the optimum solution, λ contributes less to the reference colour. On the contrary, at the beginning of the iterations, the λ provides a heavy penalty to the classification.

III. Application and Experimental Results

We implemented FCM and AFCA on a Pentium 4, CPU 3.2GHz workstation with 2 Gb memory. Figure 1a represents an original image showing a pathologic feature in mammalian heart tissue that often needs to be quantified. Hearts were excised from knockout mice known to develop dilated cardiomyopathy[6] characterised by cardiomyocyte

cell death and extensive fibrosis (i.e. deposition of collagen in damaged areas) and embedded in paraffin. Histological sections were stained with Massons trichrome that selectively stains collagens (blue), whereas cardiomyocytes and other cellular components assume a reddish colour. The amount of blue needs to be segmented and quantified. Figs. 1b and 1c show the FCM segmentation results by using 5 and 30 centroids. The latter is a more faithful representation of the original image. Figure (2) compares the segmentation results for the purple colour using FCM and AFCA. Fig. 2b matches more closely the results obtained from medical experts performing the purple colour selection manually.

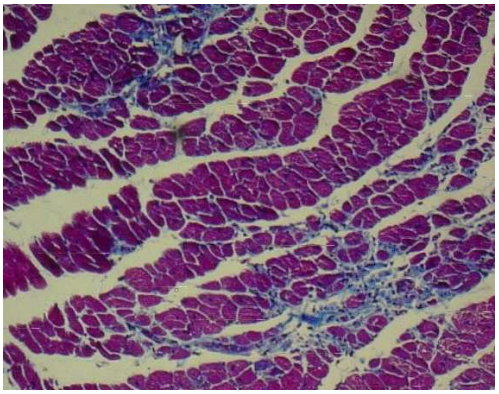

(a)Original image

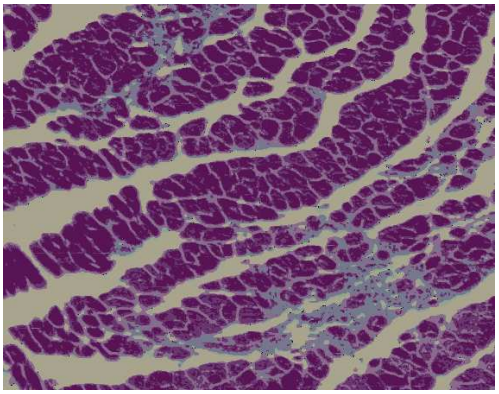

(b)FCM clustering with 5 centroids

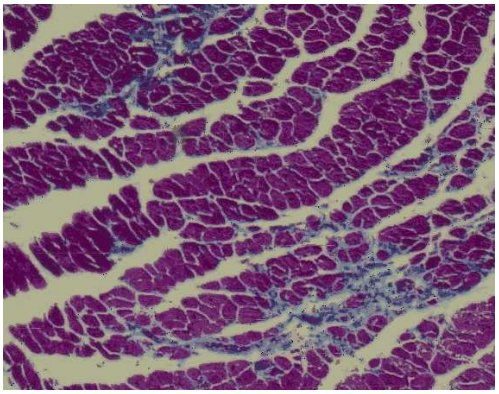

(c)FCM clustering with 30 centroids

Fig. 1. FCM classification using 5 and 30 centroids

Figure (3) presents the colour distribution in the HSB colour space. Fig. (3a) and (3b) show the original and FCM classified colour distribution in the HSB colour space. It is obvious that only 4 colours out of 30 colour centroids in (3b) relate to the stained collagens. On the contrary, in the Fig. (3c) under the regularisation of a reference colour, all of the classified colours relate to the stained collagens. Figure (4) compares the convergence plots between FCM and AFCA with different centroids. The convergence tolerance is 1.0×10^{-3}. Figs. (4a) and (4b) present the convergence curves of FCM with 30 and 5 centroids. After 20 and 11 iterations, FCM with 30 and 5 centroids reach the convergence tolerance respectively. However it takes 46 iterations to reach the same convergence tolerance using AFCA. The experiments prove that AFCA gives a slower convergence rate than traditional FCM.

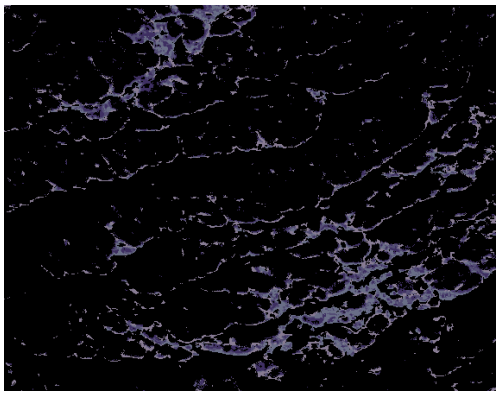

(a)Four colour centroids selected from 30 colour centroids, see Fig.1c

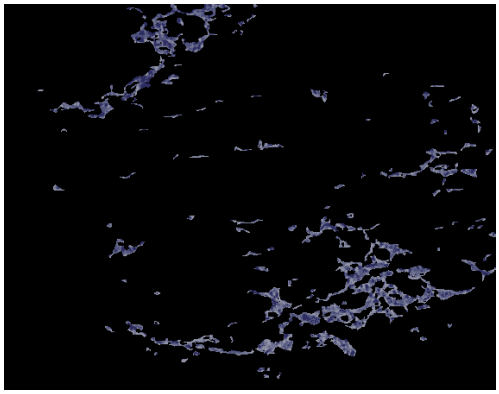

(b)AFCA segmentation results using four centroids

Fig. 2. Comparison FCM and AFCA segmentation

Figure (5) presents a cross-section of the left ventricle of a pathogenic heart. The blue colour stains the collagens that are characteristic of tissue fibrosis.

Figures (6a) and (6b) show the results of FACM segmentation using 5 and 7 centroids respectively. The segmented structure is similar in both cases, but we can see that the use of 7 centroids produces a better definition of the fibrotic network. The results of 7 centroids segmentation relate more closely to the original pathological image and match the manual analysis performed by an experienced pathologist.

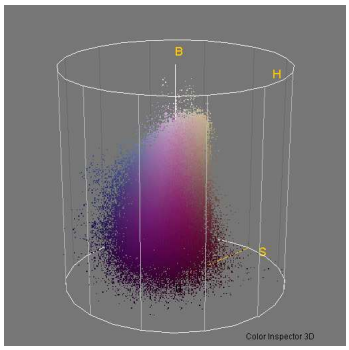

(a)Original HSB colour visualisation

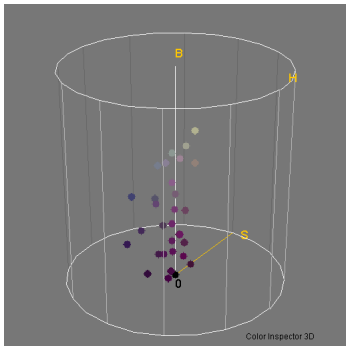

(b)30 Colour centroids using FCM

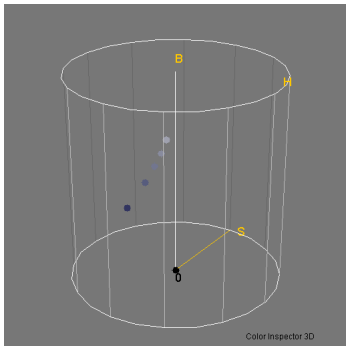

(c)5 Colour centroids using AFCA

Fig. 3. HSB colour visualisation

Table (I) compares the results between manual segmentation performed by a pathologist and our AFCA for a number of histological images.

IV. Conclusions

In this paper, we present an adaptive fuzzy C means (AFCA) algorithm to classify colours on biomedical images. In order to efficiently segment the image, a reference colour is manually selected before segmentation. Based on the hue-saturation-intensity of the reference colour, a regularisation factor Lagrange parameter, is further introduced into the AFCA. Experimental results prove that by using this algorithm, colour centroids are found with similar colour properties such as hue, saturation and intensity. In comparison to the traditional FCM, the convergent rate of the AFCA is slower for the same number of centroids.

Using our AFCA, the colour of the image is classified based on the reference colour instead of a global classification in normal FCM. Therefore using AFCA fewer centroids are needed. Since the computational complexity both AFCA and FCM is $\Theta(n^2)$ where n is the number of centroids, using fewer centroids will save on computational time. The membership matrix u is a large matrix and its size is $M \times C$, where M is the number of pixels and C the number centroids. The spatial complexity for both the AFCA and the FCM is about $\Omega(n)$ where n is the number of centroids. Using less centroids will require less memory.

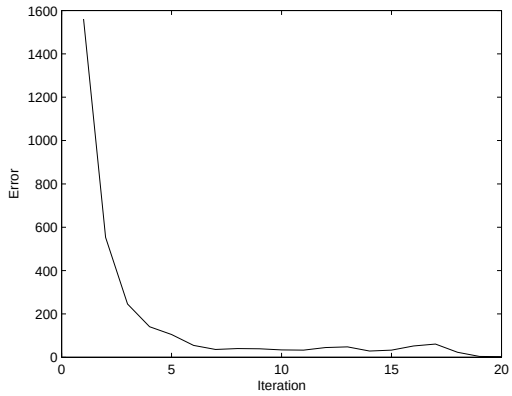

(a)Error plot of FCM, 30 centroids

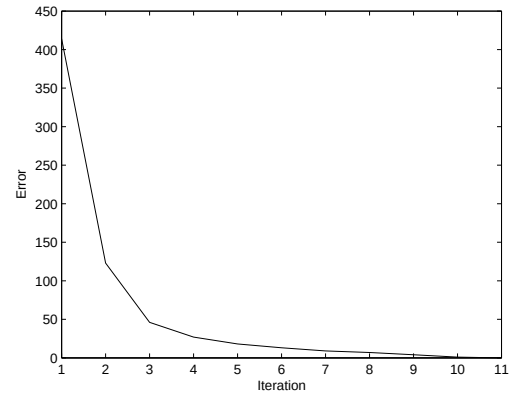

(b)Error plot of FCM, 5 centroids

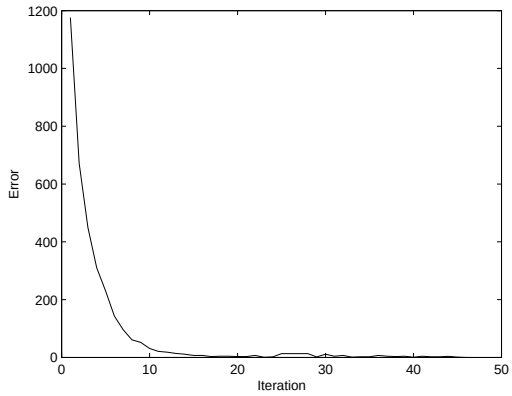

(c)Error plot of AFCA, 5 centroids

Fig. 4. Comparison of convergent plots between FCM and AFCA

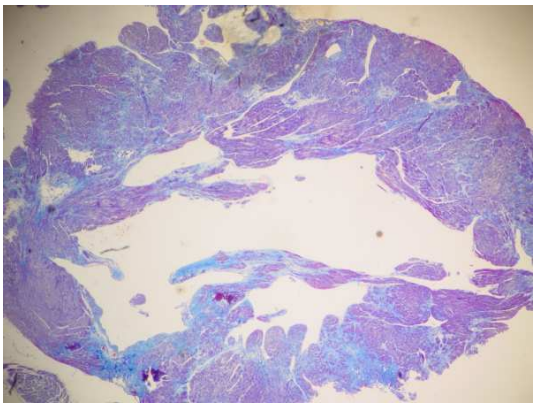

Fig. 5. Original image, section of heart showing areas of fibrosis (6.7a)

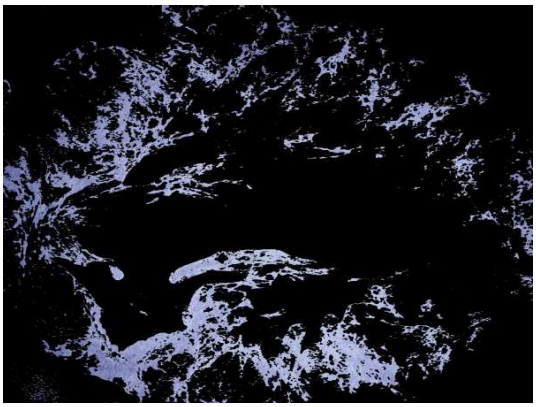

(a)AFCA segmented result using 5 centroids

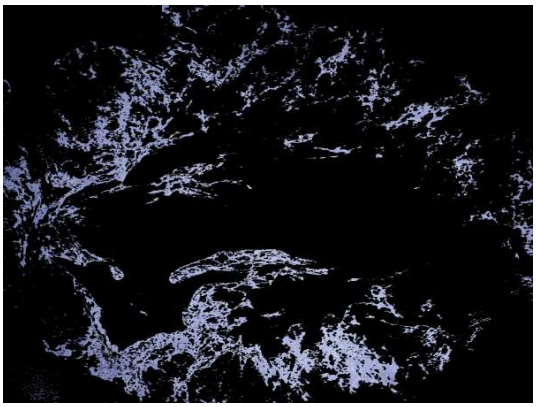

(b)AFCA segmented result using 7 centroids

Fig. 6. Comparison AFCA segmented results with different centroids

In summary, successful high resolution biomedical images segmentation is produced at less computational cost. The advantages of our AFCA algorithms are two fold, namely shorter computational time and less memory usage.

A disadvantage of both FCM and the AFCA is that the classified results depend on the initial membership matrix and the number of centroids. Unfortunately, we never know the optimum number of centroids in advance. Several different algorithms, such as principal component analysis (PCA) or subtractive clustering [5], need to be evaluated. They might improve the automatic estimation of the optimum number of centroids.

TABLE I
COMPARISON MANUAL AND AFCA SEGMENTED RESULTS

Images IDs	Manual segmentation	AFCA using 5 centroids	AFCA using 7 centroids
6.7a	17.99%	18.98%	18.03%
4.2a	1.57%	3.8%	2.8%
9.7a	7.31%	3.34%	8.0%
9.7b	4.62%	1.6%	3.56%
SC13.1b	23.1%	21.57%	22.3%

REFERENCES

[1] A.Liew, S.H.Lenung, and W.H.Lau. Segmentation of color lip images by spatial fuzzy clustering. *IEEE Transactions on Fuzzy Systems*, 11:542–549, 2003.

[2] D.L.Pham and J.Prince. Adaptive fuzzy segmentation of magnetic resonance images. *IEEE Transactions on Medical Imaging*, 18:737–751, 1999.

[3] G.Bueno, R.González, J.González, and M.García-Rojo. Fuzzy colour c-means clustering for pattern segmentation in histological images. *The 3rd European Medical and Biological Engineering Conference*, 2005.

[4] J.Puzicha, T.Hofmann, and J.M.Buhmann. Histogram clustering for unsupervised image segmentation. *IEEE Conference on Computer Vision and Pattern Recognition*, 1999.

[5] W. Liu, C. Xiao, B. Wang, Y. Shi, and S. Fang. Study on combining subtractive clustering with fuzzy c-means clustering. *Machine Learning and Cybernetics*, 5:2659– 2662, 2003.

[6] D. Milner, G. Weitzer, D. Tran, A. Bradley, and Y. Capetanaki. Disruption of muscle architecture and myocardial degeneration in mice lacking desmin. *Journal of Cell Biology*, 134:1255–1270, 1996.

[7] M.Pesaresi and J.A.Benediktsson. A new approach for the morphological segmentation of high-resolution satellite imagery. *IEEE Transactions on Geoscience and Remote Sensing*, 39:309–320, 2001.

[8] P.Felzenszwalb and D.Huttenlocher. Efficient graph-based image segmentation. *International Journal of Computer Vision*, 59, 2004.

[9] R.N.Dave and K.Bhaswan. Adaptive fuzzy c-shells clustering and detection of ellipses. *IEEE TRANSACTIONS ON NEURAL NETWORKS*, 3:643–662, 1992.

[10] S.Albayrak and F.Amasyali. Fuzzy c-means clustering on medical diagnostic systems. *The 12th International Turish Symposium on Artificial Intelligence and Neural Networks*, 2003.

[11] T.Červinka, I.Provazník, J.Hyttinen, T.Heinonen, and P.Dastidar. Pre-processing computer tomography images for segmentation based on region growing methods. *The 3rd European Medical and Biological Engineering Conference*, 2005.

[12] Y.Deng, B.Manjunath, and H.Shin. Color image segmentation. *IEEE Conference on Computer Vision and Pattern Recognition*, 1999.